# RARE-FL: Resilient Accelerated & Risk-Aware Edge Federated Learning in Scarce Data Scenario

Mohamed Ads, Member, IEEE, Hesham ElSawy, Senior Member, IEEE, Hossam S. Hassanein, Fellow, IEEE

***Abstract*—Federated learning as a Service (FLaaS) is promoted as a privacy-preserving collaborative machine learning, which is challenged by channel impairments and the scarcity of trustworthy devices in wireless networks. Assuming a trustworthy metric (TM) reflecting the reported local models accuracy, we propose a resilient, accelerated, and risk-aware edge FL (RARE-FL) that utilizes the TM scores to provide fast and trustworthy FLaaS without relying on validation datasets. The proposed RARE-FL is applied to a communication harsh 6G non-terrestrial network, where mutually interfering unmanned aerial vehicles (UAV) provide FLaaS to spatially distributed edge devices. Our numerical results on MNIST and CIFAR-10 datasets affirm the efficacy of the proposed RARE-FL, showcasing its enhanced performance and reliability over existing methodologies.**

## I. Introduction

Federated learning as a service (FLaaS) is expected to prevail in 6G [1]. Instead of learning on raw data, FL combines privately trained local models from edge devices. The fidelity of FL is subject to the amount of data, the data distribution, and the local models precision at the edge devices, which inspired several sophisticated model aggregation techniques to sustain acceptable FL performance [2]–[6]. However, the FL schemes in [2]–[6] are oblivious to the accuracy and validity of the aggregated local models. To ensure trustworthy FL, there is surging interest to validate local models before aggregation. Utilizing statistical information, Krum [7], Bulyan [8], and Trimmed-Mean [9] identify and exclude outliers based on a distance metric from the reported mean or based on a similarity metric with other reported local models. Another direction is to rank edge devices based on trustworthiness (also denoted as reputation) metrics that is developed through their previous FL contribution [10], [11]. However, the authors in [7]–[9], [11] apply binary decisions to consider/discard devices, which might not be efficient in scarce data scenarios. The work in [12], [13] develops a dynamic inclusion/exclusion criterion for the local models throughout the aggregation rounds. However, the work in [12], [13] relies on validation dataset, which might not be available at the central aggregator.

This letter proposes a resilient, accelerated, and risk-aware edge FL (RARE-FL) that utilizes trustworthy metric (TM) scores to provide fast and trustworthy FLaaS without relying on a validation dataset. Inspired by transfer learning, we formulate a novel RARE-FL aggregation function that progressively reduces the influence of edge devices in the learning process in which the magnitude of the reduction is determined by the device TM score as compared to the average TM scores across the network. The proposed TM-based progressive reduction is the key contribution of the proposed RARE-FL, which we prove necessary for a non-identically distributed (Non-IID) data-scarce environment. Wile existing techniques are focused on detecting/discarding altered local model [7]–[9], our RARE-FL leverages progressive filtering to better utilize limited data resources. Furthermore, RARE-FL follows a descending signal-to-interference-plus-noise-ratio (SINR) inclusion of edge devices to ensure accelerated convergence with fair contribution from devices. The results in a 6G non-terrestrial network underscore higher accuracy and faster convergence for RARE-FL compared to state-of-the-art models.

The authors are with the School of Computing, Queen's University, ON, Canada, e-mail: {m.ads, hesham.elsawy, hossam.hassanein}@queensu.ca

## II. System Model and Problem Formulation

*1) **FLaaS Model**:* The FLaaS is provided by unmanned aerial vehicles (UAVs), where each UAV acts as the aggregator server (AS) for $K$ proximate edge devices that possess related data for the FLaaS transaction. The proposed system considers non-hierarchical FLaaS architecture, where each UAV independently offers its FLaaS service without any inter-UAV data or model sharing. To perform the FLaaS for the $K$ proximate devices, each UAV is tasked with the execution of a distributed optimization problem, formally expressed as:

$$\min_{\boldsymbol{g}_t} f(\boldsymbol{g}_t) = \sum_{x=1}^{K} a_x F_x(\boldsymbol{g}_t), \tag{1}$$

where $a_x$ is a weighting factor for the local model aggregation that accounts for per-device parameters such as the amount of possessed data and TM score. A FLaaS transaction involves several global iterations $t \in \{0, T-1\}$, where the loss function $F_x(\cdot)$ is assessed at the global model parameter $\boldsymbol{g}_t$ for each device $x$. Hence, (1) seeks the most suitable vector $\boldsymbol{g}_t$ that minimizes the average loss across all devices $f(\cdot)$, thereby facilitating comprehensive and effective learning that is reflective of the aggregate insights derived from the network. For each iteration of the global model in (1), every device updates its local model parameters $e \in \{0, E-1\}$ times through the execution of the following update rule:

$$\boldsymbol{w}_{x,t}^{(e+1)} = \boldsymbol{w}_{x,t}^{(e)} - \zeta_x \nabla F_x(\boldsymbol{w}_{x,t}^{(e)}), \tag{2}$$

where $\boldsymbol{w}_{x,t}^{(e)}$ represents the local model of device $x$ after $e$ epochs during the $t^{\text{th}}$ global round, $\zeta$ represents the learning rate, and $\nabla F_x(\cdot)$ is the gradient of the objective function to the local model parameters. Each device transmits its final parameter vector $\boldsymbol{w}_{x,t}$ to the UAV.

*2) **Network Model**:* The proposed scheme presumes a static network for each FLaaS transaction, making it well-suited for applications that require location-specific models, such as in smart cities or precision agriculture, where a set of stationary sensors, devices, or robots are deployed. Nevertheless, UAVs are chosen as aggregators to leverage their mobility in case of location updates across different FLaaS transactions. Furthermore, UAV can establish Line of Sight (LOS) connections that enhance signal quality between edge devices and the aggregator as compared to traditional fixed-base stations. It is assumed that the UAVs are distributed according to a Poisson Point Process (PPP) at an altitude of $h$ meters. The $K$ devices of each UAV are randomly distributed within its Voronoi cell. All UAVs employ a universal frequency reuse scheme for $K$ orthogonal channels each with bandwidth $B$ Hz. Hence, intra-cell interference is eliminated, however, devices located in different Voronoi cells experience inter-cell interference. The LOS and Non-LOS (NLOS) are incorporated as in [14], where

$$P_L(r_x) = \frac{1}{1 + a\exp\left(-b\left[\frac{180}{\pi}\arctan\left(\frac{h}{d_x}\right) - a\right]\right)}, \quad (3)$$

is the LOS probability for a device located at a horizontal distance of $r_x$ from a UAV and the parameters $a$ and $b$ are environmental factors. The NLOS probability is $P_N(r_x) = 1 - P_L(r_x)$. The fading is assumed to follow a Nakagamim distribution with gamma shape parameters $M_L$ and $M_N$ for LOS and NLOS respectively. The devices and UAVs employ directional antennas, where the antenna gain is represented by $G_{nM}$ for the main lobe and $G_{ns}$ for the side lobe such that the subscript $n = x$ for the device or $n = u$ for the UAV. The antenna gains are categorized into four distinct combination patterns: $G_0 = G_{xM}G_{uM}$ with probability $\mathbb{P}_0 = \left(\frac{\theta_x}{2\pi}\right)\left(\frac{\theta_u}{2\pi}\right)$, $G_1 = G_{xs}G_{uM}$ with probability $\mathbb{P}_1 = \left(1 - \frac{\theta_x}{2\pi}\right)\left(\frac{\theta_u}{2\pi}\right)$, $G_2 = G_{xM}G_{us}$ with probability $\mathbb{P}_2 = \left(\frac{\theta_x}{2\pi}\right)\left(1 - \frac{\theta_u}{2\pi}\right)$, and $G_3 = G_{xs}G_{us}$ with probability $\mathbb{P}_3 = \left(1 - \frac{\theta_x}{2\pi}\right)\left(1 - \frac{\theta_u}{2\pi}\right)$. We assume aligned antennas for intended links $G_0$ and flawless global model feedback from a UAV to its edge devices.

*3) **Trust Model**:* The devices are assigned a TM score ($\gamma_x$) that reflects their data quality, computation precision, and/or security profile (e.g., installed security software and patches). Overall, a higher TM score reflects a more accurate local model for the required FLaaS transaction. Without loss of generality, a multiplicative alternation for the local model is employed as a function of the TM score, which is given by

$$\boldsymbol{w}'_{x,t}(\gamma_x) = \boldsymbol{w}_{x,t} \cdot \left(1 + \frac{(1-\gamma_x)}{10}\right), \quad (4)$$

to represent noisy local models that deviate slightly from the truth. The deviation magnitude in (4) is inversely proportional to the TM metric, which can be maliciously injected by stealthy adversaries or naturally arise from faulty computations, weight quantization, and model compression. In all cases, the noise in (4) can accumulate over the learning rounds and compromise the global model fidelity.

It is worth noting that this letter assumes the availability of accurate TM scores, which can be deduced from previous FLaaS transactions by testing the accuracy of FL models trained with and without the local model of each device. The details to develop TM scores are out of the scope of this letter and can be found in [10], [11].

## III. RARE-FL ALGORITHM

This section explores the FL model in (1) for the proposed RARE-FL scheme, where we define the per device weighting factor $a_x$ and utilize the following aggregation function

$$\boldsymbol{g_{t+1}} = \boldsymbol{g_t} + \sum_{x=1}^{K} \underbrace{p_x \kappa_x}_{a_x} W_{x,t} \times (\boldsymbol{w'}_{x,t}(\gamma_x) - \boldsymbol{g_t}), \quad (5)$$

where $p_x = {}^{D_x}/_{D}$, $D_x$ is the amount of data possessed at device $x$, $D = \sum_{x=1}^{K} D_x$ is the total amount of available data, $\boldsymbol{w'}_{x,t}(\gamma_x)$ is the reported local model given by (4), $W_{x,t}$ is a wireless communication factor and $\kappa_x$ is a trustworthy factor that is detailed in the sequel.

### A. Wireless Communications Factor

The aggregation function (5) is performed at the UAV and the local model update ( i.e., in (2) and (4)) is performed at the edge device. Hence, at each iteration $t$, each device needs to transmit its own local update to the UAV for aggregation. To accelerate the FL convergence, a descending transmission rate is employed with the learning phases. That is, at the $t^{\text{th}}$ round, the local model is transmitted at rate

$$\mathcal{R}_t = B\log_2(1 + \tau_t), \quad (6)$$

such that $\tau_0 > \tau_1 > \cdots > \tau_{T-1}$. Due to path loss and fading, the uplink transmission of the local model is successfully received at the UAV with probability $\mathbb{P}\{\text{SINR}_{x,t}^{(z)} > \tau_t\}$, where the instantaneous (i.e., at the $t^{\text{th}}$ round) uplink SINR is expressed as:

$$\text{SINR}_{x,t}^{(z)} = \frac{PG_0H_{z,t}\left(\sqrt{h^2 + r_x^2}\right)^{-\chi_z}}{I_L + I_N + N_0}, \quad (7)$$

where $z \in \{N, L\}$ indicates a LOS or NLOS transmission, $\chi_z$ is path loss exponent, $P$ is the uplink transmission power, $H_{z,t}$ is the instantaneous fading power gain, $N_0$ is the background noise, $I_{L_t}$ and $I_{N_t}$ are the instantaneous interference originating from LOS and NLOS communication.

Starting with high transmission rates shortens the duration of initial rounds at the cost of limiting the aggregation to high SINR devices. Proceeding with the learning phases, the transmission rate requirements are relaxed and more devices are included in the learning process to fine-tune the FL model. To ensure fair contribution from all devices, the wireless communication factor in (5) is expressed as

$$W_{x,t} = \frac{\mathbb{1}(\text{SINR}_{x,t} > \tau_t)}{\mathbb{P}\{\text{SINR}_{x,t} > \tau_t\}}, \quad (8)$$

where the numerator ensures the inclusion of only successfully transmitted models and the denominator amplifies the contribution of devices that have lower transmission success probability. Following well-celebrated stochastic geometry analysis

for uplink UAV networks [15], the distance-dependent average success probability can be obtained as

$$\begin{aligned}&\mathbb{P}\{\mathrm{SINR}_{x,t} > \tau_t\}\\&= \sum_{k=1}^{z_N} (-1)^{k+1} \binom{z_N}{k} \exp\left(-N_0 \sigma_N\right) \mathcal{L}_L\left(\sigma_N\right) \mathcal{L}_N\left(\sigma_N\right) P_N(r_x)\\&+ \sum_{k=1}^{z_L} (-1)^{k+1} \binom{z_L}{k} \exp\left(-N_0 \sigma_L\right) \mathcal{L}_L\left(\sigma_L\right) \mathcal{L}_N\left(\sigma_L\right) P_L(r_i), \quad (9)\end{aligned}$$

where $\mathcal{L}_L(\cdot)$ and $\mathcal{L}_N(\cdot)$ are the Laplace transforms (LTs) of the probability density functions of the LOS and NLOS interfering links, respectively, and $\sigma_z = \frac{g_z (r_x^2 + h^2)^{\chi z/2} \mu_t}{P G_0}$ for $z \in \{N, L\}$. Following stochastic geometry analysis for Nakagami-m fading environments [16], the LTs in (9) can be expressed as

$$\begin{aligned}\mathcal{L}_z(s) = \exp\Bigg\{ &-2\pi\lambda \sum_{q=0}^{3} \mathbb{P}_q \int_0^{\infty} \left(1 - \exp\{-\pi\lambda r^2\}\right)\\&\left(1 - \left[1 + \frac{s P G_q (q^2 + h^2)^{-\gamma_z/2}}{m_z}\right]^{-m_z}\right) q \, dq \Bigg\}.\end{aligned} \quad (10)$$

It is worth noting that the device to serving UAV distance $r_x$ in (9) can be deduced from the channel state information or channel quality index.

### B. Trustworthy Factor

The factor $W_{x,t}$ is meant to reduce the impact of wireless communication impairments ensuring accelerated and unbiased FL model aggregation. To further account for the TM scores, we implement the following trustworthy factor

$$\kappa_x = \mathbb{1}(\gamma_x > \rho) \exp\{-(1 - \gamma_x)(1 - \mu)\mathbb{P}\{\mathrm{SINR}_{x,t} > \tau_t\} t\}, \quad (11)$$

where $\rho$ is the minimum acceptable TM score and $\mu = \sum_{x=1}^{k} \frac{\gamma_x}{K}$ is the average TM score across the contributing edge devices.

The trustworthy factor in (11) is inspired by the concept of transfer-learning for scarce data scenarios [17], [18]. The inspiration stems from the utilization of transfer learning to pre-trained models (i.e., on close but not similar scenarios) that are then fine-tuned by the scarce data of the intended scenario. Such knowledge transfer has been shown to outperform overfitted models that are solely trained via the scarce data of the intended scenario. We can project the same criterion to our use case by considering that transfer learning is initialized with distorted data (i.e., the data of the pre-trained model) and is fine-tuned by accurate data (i.e., data of the intended scenario). On the same line of thought, devices with lower TM scores are included at initial training rounds to accelerate convergence and avoid overfitting while devices with higher TM scores are used for fine-tuning. Based on the TM score, the exponentially decaying factor $\exp\{1 - (1 - \gamma_x)(1 - \mu)\mathbb{P}\{\mathrm{SINR}_{\mathrm{x,t}} > \tau_t\} t\}$ is crafted to gradually diminish the influence of distorted models in a proportion that is relative to their TM score, which reflects the magnitude of model distortion. Such progressive elimination exploits all the available data while keeping devices with higher TM scores (i.e., more accurate data) for more iterations that fine-tune the model and improve the overall accuracy. Nevertheless, (11) utilizes the indicator function $\mathbb{1}(\gamma_x > \rho)$ to completely exclude devices with intolerably low TM scores (i.e., highly distorted local models) from the aggregation function to avoid steep FL accuracy divination.

Different from transfer learning, the proposed RARE-FL has no hard boundary between the pre-training and fine-tuning phases. In contrast, the RARE-FL presents a per-device soft transition between the pre-training and fine-tuning phases via the trustworthy factor in (11). In particular, the four components that determine the per-iteration contribution of each device in the FLaaS transaction are detailed below

1) **Per-device TM Factor:** The per-device factor $(1 - \gamma_x)$ reflects the magnitude of distortion of the reported local model. Hence, devices with lower TM scores are eliminated faster to ensure that devices with more accurate local models have greater influence on the fine-tuned FL model. Note that fully trusted $\gamma_x = 1$ devices are never eliminated from (11).
2) **Universal TM Factor:** A lower $\mu$ implies, on average, more distorted local models among the edge devices. Hence, the universal factor (1-$\mu$) ensures a faster transition from pre-training to fine-tuning for scenarios with higher distortions in local models (i.e., lower $\mu$), and vice versa. The universal TM factor is computed at the UAV as $\mu = \sum_{x=1}^{k} \frac{\gamma_x}{K}$ to determine average trust metric across all users in the network. The value of $\mu$ reflects the overall trustworthiness of the network to determine the relative accuracy of the local models reported by each device.
3) **Per-device Participation Factor:** The factor $(\mathbb{P}\{\mathrm{SINR}_{x,t} > \tau_t\} \times t)$ accounts for the distant-dependent probability of success for the local model transmissions. Hence, accounting for the successful participation of each device in the global rounds rather than the absolute iteration index.
4) **The Indicator Function** The factor $\mathbb{1}(\gamma_x > \rho)$ excludes devices with highly distorted local models to avoid steep accuracy divination.

### C. The RARE-FL Algorithm

The RARE-FL algorithm, as detailed in Algorithm 1, orchestrates dynamic and robust FLaaS transactions. The algorithm starts with an initial global model $\boldsymbol{g}_0$ sent from a UAV to all $K$ devices to commence local training using (2). Then, devices transmit their local models back to the UAV as in (4). At the UAV, devices are included in the aggregation to update the global model according to the weights defined in (5). Hence, mitigating potential deviation due to wireless channel impairments and local model distortions, which guarantees resilient, trustworthy, and accurate FLaaS transactions.

It is worth mentioning that, by virtue of the aggregation function in (5) with the trustworthy factor defined in (11), **Algorithm 1** is self-sufficient. Different from the trustworthy FL reported in [12], [13], the UAV for the proposed RARE-FL does not need to possess a validation dataset to either validate

This article has been accepted for publication in IEEE Wireless Communications Letters. This is the author's version which has not been fully edited and content may change prior to final publication. Citation information: DOI 10.1109/LWC.2024.3469557

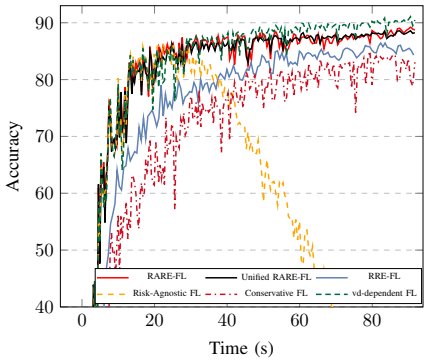


Fig. 1. MNIST Accuracy vs time ($\mu = 0.7$)

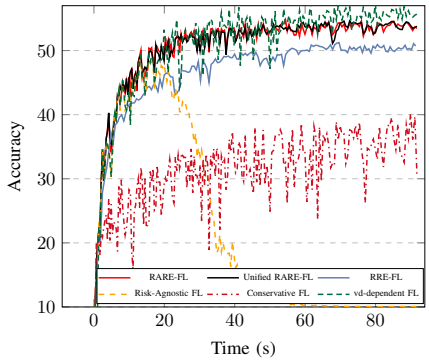


Fig. 2. CIFAR-10 Accuracy vs time ($\mu = 0.85$)

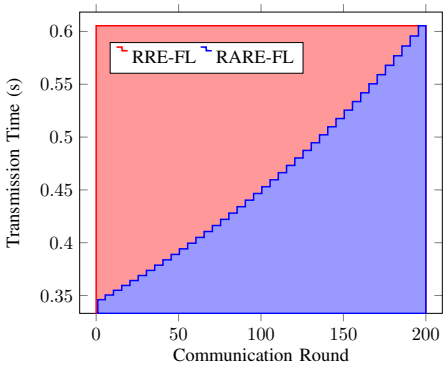


Fig. 3. RARE-FL vs RRE-FL Tx time

**Algorithm 1:** RARE-FL Algorithm

**Data:** $T, \mu, \tau_t, \theta_i, E, \zeta_x, \gamma_x$
**Result:** $\boldsymbol{g}_t$
Initialization $t \leftarrow 0$;
$\boldsymbol{g}_0 \leftarrow$ Initial Model;
**while** $t < T$ **do**
  $x \leftarrow 1$ **while** $x \leq K$ *for each client* **do**
    $\boldsymbol{w}_{x,t}^{(0)} \leftarrow \boldsymbol{g}_t$;
    $e \leftarrow 0$;
    **while** $e \leq E-1$ **do**
      $\boldsymbol{w}_{x,t}^{(e+1)} \leftarrow \boldsymbol{w}_{x,t}^{(e)} - \zeta_x \nabla F_x(\boldsymbol{w}_{x,t}^{(e)})$;
      $e \leftarrow e+1$
    **end**
    $\boldsymbol{w}'_{x,t} \leftarrow \boldsymbol{w}_{x,t}^{(E)} \cdot \left(1 + \frac{(1-\gamma_x)}{10}\right)$;
    transmit $\boldsymbol{w}'_{x,t}$;
    $x \leftarrow x+1$;
  **end**
  **At the BS:**
  $\boldsymbol{g}_{t+1} \leftarrow \boldsymbol{g}_t + \sum_{x=1}^{K} p_x \kappa_x W_{x,t} \times (\boldsymbol{w'}_{x,t}(\gamma_x) - \boldsymbol{g}_t)$;
  $t \leftarrow t+1$
**end**
**return** Result;

the reported local models or to track the convergence of the global model.

## IV. Numerical Results

The FLaaS is implemented on a non-terrestrial network in which the locations of the UAVs are generated via a 2-D Poisson Point Process with intensity ($\lambda$) 50/km$^2$ located at a height ($h$) of 45m on an area of 3000 $\times$ 3000 km$^2$. The UAVs are equipped with RBs each allowing them to serve up to $K = 30$ concurrent devices. The devices operate over $B = 1$ MHz channels with an uplink transmission power of 10 dBm. For signal propagation, the path loss exponent is set to be $\chi_N = 4$ for NLoS and $\chi_L = 2.5$ for LoS links. The transmission of both UAVs and devices is characterized by a main lobe beamwidth ($\theta$) of 40 degrees with a main lobe gain of 5 dBi and a side lobe gain of 0 dBi. For accelerated FLaas, a descending SINR threshold $\tau_t$ is employed in the range from 5 dB to 1 dB with a step size of -0.1 dB. For the trustworthiness landscape, we consider $K_t$ fully trusted devices (i.e., with unity TM score) and $K_r = K - K_t$ risky devices with TM scores randomly drawn from a beta distribution with shape and scale parameters $\alpha$ and $\beta$ and only accommodating risky users with $\rho > 0.3$. To demonstrate the RARE-FL performance, two scenarios with varying trustworthiness levels are presented. In particular, a TM mean of $\mu = 0.7$ ($K_t = 10$, $K_r = 20$, $\alpha = 10$, $\beta = 3.75$) represents an environment with more scarce trustworthy devices than that with mean of $\mu = 0.85$ ($K_t = K_r = 15$, $\alpha = 10$, $\beta = 2$). Our architecture leverages the MNIST and CIFAR-10 datasets [19], the standard benchmarks in machine learning, to train a Convolutional Neural Network (CNN). In our experiments, the data-scarce scenario was simulated by sorting then dividing the MNIST and CIFAR-10 datasets into 60 and 50 subsets respectively with each device randomly assigned two different subsets. This setup ensures that each device has data from only two distinct classes, thereby emphasizing a situation where data is limited and non-overlapping across devices. The training consists of one epoch per round for each participant with local model size of 90 kB. We benchmark the proposed RARE-FL against the following approaches:

- **Risk-Agnostic FL**: an aggressive strategy employing an aggregation function oblivious to the TM scores by setting $\kappa_x = 1$. Hence, equally combining accurate and inaccurate local models.
- **Conservative FL**: a strategy employing a binary inclusion/exclusion rule to consider only fully trusted devices in the aggregation function by setting $\kappa_x = \mathbb{1}\{\gamma_x = 1\}$. Hence, completely avoiding inaccurate local models.
- **Validation-dataset (VD) dependent FL**: a strategy introduced in [13] that utilizes a validation dataset to keep track of the global model convergence and exclude risky devices upon model accuracy degradation.
- **Two variants of RARE-FL:**
  1) **Unified RARE-FL**: This strategy eliminates the per-device success probability from (11) and utilizes the trustworthy factor $\kappa_x = \mathbb{1}(\gamma_x > \rho) \exp\{-(1-\gamma_x)(1-\mu)t\}$ that is function of the absolute iteration index $t$. Hence, emphasizing the importance of fair device participation across the global rounds.
  2) **RRE-FL**: This is a resilient risk-aware edge (RRE) FL that operates at the minimum SINR-level allowing cell-edge devices to participate in all global

rounds. Hence, explicitly emphasising the impact of the descending SINR allocation for accelerated convergence.

Our algorithm and its variants are implemented on MNIST as in Fig. 1 and CIFAR-10 as in Fig. 2, which demonstrate that RARE-FL and its variants outperform the conservative and risk-agnostic schemes. On one hand, the conservative scheme achieves low accuracy due to the scarcity of data. On the other hand, the risk-agnostic scheme shows good initial accuracy followed by a steep accuracy degradation due to the accumulated effect of distorted local models. The declined global model accuracy of the risk-agnostic scheme can be deduced from (4), which shows a deviation from the truthful local model with a magnitude that is inversely proportional to $\gamma_x$. Due to data-scarcity, in the initial rounds, the benefit from the devices data is more prominent than the reported model deviation. However, in later rounds, the accumulated model deviations dominate and lead to an overall degradation of the global model. Hence, at later FL rounds, the devices with lower TM scores should be filtered out, which underscores the superiority of RARE-FL over the risk-agnostic approach.

By virtue of the proposed aggregation function in (11), the proposed RARE-FL benefits from all of the available data to avoid overfitting while keeping only accurate models for fine-tuning to achieve high accuracy. The VD-dependent scheme shows slightly higher accuracy than the proposed RARE-FL, which is no surprise given the assumption of the available validation dataset at the UAV. A validation dataset enables continuous monitoring of the global model accuracy and optimal switching between initial training and fine-tuning phases. Nonetheless, the availability of the validation dataset can be questionable in many scenarios.

Figs. 1 and 2 show slower convergence of the other variants compared to RARE-FL, which quantifies the impact of the dynamic SINR allocations. Interestingly, the RRE-FL also shows lower accuracy, which is due to involving larger number of risky devices per global round. The Unified RARE-FL shows slightly lower accuracy than the RARE-FL due to the fact that farther devices contribute less to the overall learning. Due to the dynamic SINR allocation, farther devices are included at later iterations (i.e., high $t$) of the RRE-FL, which entails lower contribution to the aggregation due to the exponentially decaying trustworthy factor $\kappa_t$ in the iteration round $t$.

Fig. 3 emphasises the impact of descending SINR allocation on the convergence speed. It shows the time required to transmit the local model at rate $B\log_2(1+\tau_t)$ in the uplink to the UAV. For the RARE-FL, the descending $\tau_0 < \tau_1 < \cdots < \tau_t < \cdots < \tau_{T-1}$ implies shorter transmission times for the initial rounds as shown in the blue staircase curve of Fig. 3. On the other hand, the RRE-FL utilizes the minimum $\tau_{T-1}$ for all rounds for inclusive devices contribution across all aggregation rounds, which shows a constant transmission time in Fig. 3. By virtue of the dynamic transmission time for the local models, the RARE-FL shows the faster convergence and high accuracy reported in Figs. 1 and 2.

## V. Conclusion

This letter introduces a resilient, accelerated, and risk-aware edge FL (RARE-FL) that relies on trustworthy metric (TM) to progressively scale down the contributions of edge devices in the learning process. Inspired by transfer learning, RARE-FL exploits all models for initial training to accelerate convergence and avoid overfitting while fine-tuning with trustworthy models to improve the overall accuracy. The proposed RARE-FL also reduces the impact of wireless communication impairments to ensure an accelerated and unbiased global model. Validated over MNIST and CIFAR-10 datasets in a 6G unmanned aerial vehicles (UAV) network, RARE-FL demonstrates superior performance compared to conventional schemes.

## References


[1] H. Yang, J. Zhao, Z. Xiong, K.-Y. Lam, S. Sun, and L. Xiao, "Privacy-preserving federated learning for uav-enabled networks: Learning-based joint scheduling and resource management," 2020.

[2] B. McMahan, E. Moore, D. Ramage, S. Hampson, and B. A. Arcas, "Communication-Efficient Learning of Deep Networks from Decentralized Data," in *Proceedings of the 20th International Conference on Artificial Intelligence and Statistics*, 2017.

[3] T. Li, A. K. Sahu, M. Zaheer, M. Sanjabi, A. Talwalkar, and V. Smith, "Federated optimization in heterogeneous networks," 2020.

[4] M. Salehi and E. Hossain, "Federated learning in unreliable and resource-constrained cellular wireless networks," *IEEE Trans. Commun*, 2021.

[5] R. Zhagypar, N. Kouzayha, H. ElSawy, H. Dahrouj, and T. Y. Al-Naffouri, "Characterization of the global bias problem in aerial federated learning," *IEEE Wireless Communications Letters*, 2023.

[6] H. Xia, Y. Li, C. Liu, and Y. Zhu, "Stochastic client scheduling with dynamic SINR thresholds for fast federated learning," in *2022 International Conference on Communications in China (ICCC)*, 2022.

[7] P. Blanchard, E. M. El Mhamdi, R. Guerraoui, and J. Stainer, "Machine learning with adversaries: Byzantine tolerant gradient descent," in *Advances in Neural Information Processing Systems*. Curran Associates, Inc., 2017.

[8] E. M. El Mhamdi, R. Guerraoui, and S. Rouault, "The hidden vulnerability of distributed learning in Byzantium," in *Proceedings of the 35th International Conference on Machine Learning*, 2018.

[9] D. Yin, Y. Chen, R. Kannan, and P. Bartlett, "Byzantine-robust distributed learning: Towards optimal statistical rates," in *Proceedings of the 35th International Conference on Machine Learning*, 2018.

[10] A. Gholami, N. Torkzaban, and J. S. Baras, "Trusted decentralized federated learning," in *2022 IEEE 19th Annual Consumer Communications & Networking Conference (CCNC)*, 2022.

[11] Z. Yin, K. Li, and H. Bi, "Trusted multi-domain DDoS detection based on federated learning," *Sensors*.

[12] C. Mazzocca, N. Romandini, M. Mendula, R. Montanari, and P. Bellavista, "Truflaas: Trustworthy federated learning as a service," *IEEE Internet of Things Journal*, 2023.

[13] M. Ads, H. ElSawy, and H. S. Hassanein, "Risk-aware accelerated wireless federated learning with heterogeneous clients," in *IEEE International Conference on Communications (ICC), 2024*.

[14] A. Al-Hourani, S. Kandeepan, and S. Lardner, "Optimal LAP altitude for maximum coverage," *IEEE Wireless Communications Letters*, 2014.

[15] Y. Nabil, H. ElSawy, S. Al-Dharrab, H. Attia, and H. Mostafa, "Ultra-reliable device-centric uplink communications in airborne networks: A spatiotemporal analysis," *IEEE Trans. Veh. Technol.*, 2023.

[16] H. ElSawy, E. Hossain, and M. Haenggi, "Stochastic geometry for modeling, analysis, and design of multi-tier and cognitive cellular wireless networks: A survey," *IEEE Communications Surveys & Tutorials*, 2013.

[17] A. M. Nagib, H. Abou-Zeid, and H. S. Hassanein, "Safe and accelerated deep reinforcement learning-based O-RAN slicing: A hybrid transfer learning approach," *IEEE J. Sel. Areas Commun.*, 2024.

[18] T. Balachandran, T. Abreu, M. Naloufi, S. Souihi, F. Lucas, and A. Janne, "IoT and transfer learning based urban river quality prediction," in *2022 IEEE Global Communications Conference (GLOBCOM)*, 2022.

[19] Y. Lecun, L. Bottou, Y. Bengio, and P. Haffner, "Gradient-based learning applied to document recognition," *Proc. IEEE*, 1998.